

Block-Jacobi sweeping preconditioners for optimized Schwarz methods applied to the Helmholtz equation

Ruiyang DAI¹

¹Laboratoire J.L. Lions, Sorbonne Université, 4 place Jussieu, 75005 Paris, France,
ruiyang.dai@upmc.fr

Abstract

The parallel performances of sweeping-type algorithms for high-frequency time-harmonic wave problems have been recently improved by departing from standard layer-type domain decomposition and introducing a new sweeping strategy on a checkerboard-type domain decomposition, where sweeps can be performed more flexibly. These sweeps can be done by a certain number of steps, each of which provides the necessary information from subdomains on which solutions have been obtained to their next neighboring subdomains. Although, subproblems in these subdomains can be solved concurrently at each step, the sequential nature of the process of the sweeping approaches still exists, which limits their parallel performances. Moreover, the sweeping approaches can be interpreted as a completely approximate LU factorization, which implies a huge computation cost. We propose block-Jacobi sweeping preconditioners, which are improved variants of sweeping-type preconditioners. The new feature of these improved variants can be interpreted as several partial sweeps, which can be performed parallelly. We present several two- and three-dimensional finite element results with constant and various wave speeds to study and compare the original and block-Jacobi sweeping preconditioners.

Contents

1	Introduction	2
2	Non-overlapping domain decomposition method	3
2.1	Transmission conditions	4
3	Preconditioned interface problem	4
3.1	Interface problem	5
3.2	Iterative algorithm	6
3.3	Sweeping preconditioners	6
3.3.1	Block matrix forms	6
3.3.2	Symmetric Gauss-Seidel (SGS) preconditioner	7
3.3.3	Double Sweep (DS) preconditioner	7
3.4	Block-Jacobi sweeping preconditioners	8
4	Numerical results	9
4.1	Scattering model in 2D	10
4.2	Marmousi model	12
4.3	Scattering model in 3D	14
5	Conclusion	15

1 Introduction

Solving Helmholtz problems using finite element-type methods is a tough challenge because the resulting linear systems are huge, indefinite, and ill-conditioned, which can not be handled by employing classical direct or iterative solvers. To solve the resulting linear systems, some new numerical methods are being developed: direct methods such as multi-frontal solvers, which are variants of Gauss elimination and have been applied to Helmholtz problems [2, 29]; preconditioned iterative methods such as multigrid methods and shifted-Laplacian methods, in which the inversion of preconditioners is approximated by a direct solver or an iterative solver [8, 14, 16]; domain decomposition (DD) methods, which are proposed as an alternative to combining direct and iterative methods [26]. In this paper, we focus on DD methods.

There are several types of DD methods, whose general philosophy is the same: splitting the original problem into some smaller problems on subdomains and exploiting these subproblems to construct an iterative or direct method to coordinate the solution among subdomains. DD methods can be thought of as ways to construct preconditioners for use in an iterative method, both in parallel and sequentially, such as the multiplicative Schwarz method and additive Schwarz method. However, the resulting preconditioned iterative methods are not scalable because the number of iterations grows as the frequency or the number of subdomains increases. To deal with this issue, coarse spaces viewed as a component are added to the iterative methods, which are second-level preconditioners that allow the global information exchange among all subdomains rather than local information exchange from one subdomain to its neighbors. DD methods can also yield sweeping-type algorithms [7, 12, 13, 18, 25, 30, 31]. These algorithms are motivated by physics and developed using Green's function techniques. The original domain, always considered to be a square in 2D or a cube in 3D, is decomposed into several subdomains, such as slices, squares in 2D, or cubes in 3D. The near-field solution in one subdomain is mapped to the far-field in neighboring subdomains first and propagates to all subdomains finally. These algorithms can be used as direct solvers and provide the solution with relatively high L^2 -error (see numerical results in [18]). They can also be employed as preconditioners for classical iterative methods, which can be interpreted as an approximate LU factorization of the original resulting system. There is the other family of DD methods that is non-overlapping optimized Schwarz (OS) methods. Non-overlapping Schwarz methods were introduced by P.-L. Lions [19] for the Laplace equation and proven to converge for the Helmholtz equation by B. Després [10]. Unfortunately, these methods were not practical in real applications because of their poor rate of convergence. To increase the efficiency of these methods, it has been proposed to employ more general boundary conditions for non-overlapping DD methods, which are called non-overlapping OS methods. Considerable efforts have been made to develop more accurate transmission conditions. OS methods were introduced by M. J. Gander *et al.* [15], where the zeroth-order operator is replaced by a second-order approximation of the nonlocal Dirichlet-to-Neumann (DtN) map, with coefficients to be optimized a priori depending on the geometrical configuration of the subdomains and the frequency. Later, quasi-optimal OS methods were proposed by Y. Boubendir *et al.* [6], by using a rational approximation of the nonlocal DtN. Although non-overlapping OS methods can be applied as a direct solver, they are presented, under most circumstances, as a fixed point scheme and recast into a linear system with supplementary unknowns on interfaces, which benefits from a Krylov acceleration. Recently, there are some competing non-overlapping OS methods with quite good convergence, including, but not limited to [6, 21, 22]. Although optimized transmission conditions improved the rate of convergence of non-overlapping OS methods, the number of iterations of the linear system accelerated by the Krylov method will grow as the number of subdomains increases, especially for layer-type domain decompositions. In this research context, this limitation has been adequately addressed for OS methods with layer-type domain decompositions at the level of the rate of convergence. Considered a linear system reformulated in terms of supplementary unknowns on the boundaries between the subdomains, it is natural to look for a preconditioner that accelerates the convergence of the solver. Inspired by this idea, A. Vion and C. Geuzaine proposed a double sweep preconditioner for OS methods [27], which is designed by approximating the inverse of the iteration operator, and an improved preconditioner [28] based on well-known algebraic techniques (Gauss-Seidel). However, these two sweeping preconditioners for OS methods are under lack of parallel scalability arising due to the intrinsically sequential operations and accurate and consistent information transfer between subdomains which leads to the restriction of the layer-type domain decompositions.

To address this issue, it is necessary to consider more general domain decompositions. Recently,

the parallel performances of sweeping-type algorithms have been recently improved by departing from standard layer-type domain decomposition and introducing a new sweeping strategy on checkerboard-type domain decomposition, such as L-sweeps preconditioners [25] and trace transfer-based diagonal sweeping preconditioners [18] for the Helmholtz equation, which are proposed in the context of the method of polarized traces and the source transfer method, respectively, and multidirectional sweeping preconditioners [9] for the OS methods applied to the Helmholtz equation, with high-order transmission conditions and cross-point treatments [6, 21]. The key to improving the parallelism of these algorithms is a consistent information transfer among subdomains. Therefore, several processes can be performed concurrently.

There are two strategies to assign subdomains to MPI ranks for sweeping-type algorithms: row- or column-based assignments of subdomains to MPI ranks (each row or column of subdomains is assigned to one MPI rank) and one-to-one assignments of subdomains to MPI ranks (one subdomain is assigned to one MPI rank). Using row- or column-based assignments, L-sweeps preconditioners and trace transfer-based diagonal sweeping preconditioners can be applied optimally in parallel, and they can be further parallelized by pipelining over the multiple right-hand sides with one-to-one assignments (see [18, 25]). Although it is also applicable to multidirectional sweeping preconditioners with row- or column-based assignments, it is hard to judge its effectiveness in pipelining with one-to-one assignments. The reason is that, at each iteration of the Krylov method applied to non-overlapping OS methods, the subproblems are solved twice in the matrix-free product and preconditioning procedure, respectively. For the non-overlapping OS methods with good transmission conditions that have a high convergence rate, with sweeping-type preconditioners, the cost of the preconditioning procedure which might be much higher than that in the matrix-free product could deteriorate the efficacy. On the contrary, there isn't this issue in sweeping-type algorithms for the Helmholtz equation because the matrix-free product in these algorithms is only matrix-vector multiplications. Therefore, in this paper, we only discuss sweeping-type preconditioners with row- or column-based assignments.

While the algorithms with row- or column-based assignments possess much better parallel performances compared to the layer-by-layer sweeping algorithm, there are still some limitations. Firstly, each step of sweeps is still a sequential process, which leads to a long preconditioning procedure compared to the matrix-free-product phase. Next, the starting point of sweeping preconditioning is from one subdomain which causes some waste of computation resources. At last, the current sweeping approaches can be interpreted as a completely approximate LU factorization, which implies a high computation cost.

In this work, we propose block-Jacobi sweeping preconditioners, which are improved variants of sweeping-type preconditioners. The new feature of these improved variants can be interpreted as overlapping block-Jacobi preconditioners for a block form matrix of the interface problem. Thanks to the introduction of the block-Jacobi-type matrix, full sweeps are decomposed into several partial sweeps, which can be performed concurrently. These novel sweeping preconditioners provide enhanced scalability and make full usage of the resources on parallel computer architectures.

This paper is organized as follows. In Section 2, the non-overlapping domain decomposition method for Helmholtz problems is presented. Then, the preconditioned iterative scheme with full sweeping preconditioners and block-Jacobi sweeping preconditioners is presented in Section 3. Next, Section 4 shows several two- and three-dimensional finite element results with constant and various wave speeds to study and compare the original and block-Jacobi sweeping preconditioners. Finally, conclusions are drawn in Section 5.

2 Non-overlapping domain decomposition method

We consider the two- or three-dimensional Helmholtz equation in a regular domain Ω (for the sake of simplicity, Ω is considered to be a square or a cube) with a Sommerfeld absorbing boundary condition (ABC) on the boundary Γ^∞ of Ω . We seek the field $u(\mathbf{x}) \in H^1(\Omega)$ that verifies

$$\begin{cases} (-\Delta - \kappa^2)u = f, & \text{in } \Omega, \\ (\partial_{\mathbf{n}} - \nu\kappa)u = g, & \text{on } \Gamma^\infty, \end{cases} \quad (1)$$

where $f \in L^2(\Omega)$ and $g \in L^2(\Omega)$ are the sources terms, κ is the wavenumber, $\partial_{\mathbf{n}}$ is the exterior normal derivative. We take the convention that the time-dependence of the fields is $e^{-i\omega t}$, where ω is the angular frequency and t is the time.

We consider a non-overlapping partition of the domain Ω , which is decomposed into a finite number N_{dom} of open subdomains denoted as Ω_i , that is

$$\bar{\Omega} = \bigcup_{i=1}^{N_{\text{dom}}} \bar{\Omega}_i, \quad \text{and} \quad \Omega_i \cap \Omega_j = \emptyset \quad \text{for} \quad j \neq i.$$

The boundary of a subdomain Ω_i is split into two parts: the exterior part $\partial\Omega_i \cap \Gamma$ and the interior part including decomposed interior boundaries $\Gamma_{ij} := \partial\Omega_i \cap \partial\Omega_j$. The domain decomposition method consists in considering the N_{dom} local sub-problems: Seek the field $u(\mathbf{x}) \in H^1(\Omega)$ that verifies

$$\begin{cases} (-\Delta - \kappa^2)u_i = f, & \text{in } \Omega_i, \\ (\partial_{\mathbf{n}_i} - i\kappa)u_i = g, & \text{on } \partial\Omega_i \cap \Gamma^\infty, \end{cases} \quad (2)$$

which are equivalent to the Helmholtz equation if these sub-problems are coupled by the two transmission conditions (Dirichlet and Neumann conditions) at the interior boundaries Γ_{ij}

$$\begin{cases} u_i = u_j, & \text{on } \Gamma_{ij}, \\ \partial_{\mathbf{n}_{ij}}u_i = -\partial_{\mathbf{n}_{ji}}u_j, & \text{on } \Gamma_{ij}, \end{cases} \quad (3)$$

where $\partial_{\mathbf{n}_{ij}}$ is the exterior normal derivative from Ω_i to Ω_j at the interface Γ_{ij} .

For improving the rate of convergence of the algorithms above, we need to introduce an impedance operator T [6] and take two linear combinations of Dirichlet and Neumann conditions. Using these Robin conditions, we can rewrite the decomposed problem in the form of the coupled local sub-problems

$$\begin{cases} (-\Delta - \kappa^2)u_i = f, & \text{in } \Omega_i, \\ (\partial_{\mathbf{n}_i} - i\kappa)u_i = g, & \text{on } \partial\Omega_i \cap \Gamma^\infty, \\ (\partial_{\mathbf{n}_{ij}} - i\kappa T)u_i = (-\partial_{\mathbf{n}_{ji}} - i\kappa T)u_j, & \text{on } \Gamma_{ij}, \forall j \in D_i, \end{cases} \quad (4)$$

where the set

$$D_i := \{j \in \{1, \dots, N_{\text{dom}}\} \text{ such that } j \neq i \text{ and } \Gamma_{ij} \neq \emptyset\}.$$

2.1 Transmission conditions

In this paper, we employ transmission conditions based on high-order absorbing boundary conditions (HABCs), which lead to an excellent approximation of the outgoing waves for layered-type domain decompositions and checkerboard-type domain decompositions [6, 21]. For more general partitions, there are transmission conditions based on second-order absorbing boundary conditions [11]. When these transmission conditions are employed on the polygonal domains, special treatment at corners in 2D cases and edges and corners in 3D cases is required, which promises the high-fidelity solution.

In Section 4, we employ these high-quality boundary conditions. But in the following section, where we study the algebraic structure of the interface problem, we consider a setting with boundary conditions based on the basic impedance operator for the sake of clarity.

3 Preconditioned interface problem

To derive the interface problem, let's introduce $w_i \in H^1(\Omega_i)$ a lifting of the source: Seek $w_i \in H^1(\Omega_i)$ that verifies

$$\begin{cases} (-\Delta - \kappa^2)w_i = f, & \text{in } \Omega_i, \\ (\partial_{\mathbf{n}_i} - i\kappa)w_i = g, & \text{on } \partial\Omega_i \cap \Gamma^\infty, \\ (\partial_{\mathbf{n}_{ij}} - i\kappa T)w_i = 0, & \text{on } \Gamma_{ij}, \forall j \in D_i. \end{cases} \quad (5)$$

By the linearity of the problem, the field u_i can be decomposed into $v_i + w_i$, where v_i is the field (4) after lifting the sources by (5).

3.1 Interface problem

We introduce the local scattering operator:

$$S_{ij} : x_{ik} \rightarrow (-\partial_{\mathbf{n}_{ij}} - \nu\kappa T)v_i \quad \text{where} \quad \begin{cases} (-\Delta - \kappa^2)v_i = 0, & \text{in } \Omega_i, \\ (\partial_{\mathbf{n}_i} - \nu\kappa)v_i = 0, & \text{on } \partial\Omega_i \cap \Gamma^\infty, \\ (\partial_{\mathbf{n}_{ik}} - \nu\kappa T)v_i = x_{ik}, & \text{on } \Gamma_{ik}, \\ (\partial_{\mathbf{n}_{il}} - \nu\kappa T)v_i = 0, & \text{on } \Gamma_{il}, \forall l \neq k, \end{cases} \quad (6)$$

where $j, k, l \in D_i$.

Using the linearity of the problem and the above scattering operator, we obtain the interface problem

$$(\partial_{\mathbf{n}_{ji}} - \nu\kappa T)v_j = \sum_{k \in D_i} S_{ij}(\partial_{\mathbf{n}_{ik}} - \nu\kappa T)v_i + (-\partial_{\mathbf{n}_{ij}} - \nu\kappa T)w_i, \quad j \in D_i.$$

We introduce the global scattering operator $\mathbf{S} \in \mathcal{M}_{2N_{\text{dom}}}(S_{ij})$, the global additional variable vector $\mathbf{g} \in \mathcal{V}_{2N_{\text{dom}}}(g_{ij})$, and the global right-hand-side vector $\mathbf{b} \in \mathcal{V}_{2N_{\text{dom}}}(b_{ij})$, where

$$\begin{aligned} g_{ij} &= (+\partial_{\mathbf{n}_{ij}} - \nu\kappa T)v_i, \\ b_{ji} &= (-\partial_{\mathbf{n}_{ij}} - \nu\kappa T)w_i. \end{aligned}$$

We order the elements in the global vector with the Cartesian product $\mathbb{D} \times \mathbb{D}$ which is the set of all ordered pairs of elements from \mathbb{D} , where $\mathbb{D} = \{1, 2, \dots, N_{\text{dom}}\}$. So we obtain that \mathbf{g} is the solution to

$$(\mathbf{Id} - \mathbf{S})\mathbf{g} = \mathbf{b}, \quad (7)$$

or

$$g_{ji} - \sum_k S_{ij}g_{ik} = b_{ji}, \quad \forall j \in \mathbb{D}, \text{ for } i, k \in D_j. \quad (8)$$

We show an example below:

$$\begin{bmatrix} g_{12} \\ g_{13} \\ g_{21} \\ g_{23} \\ g_{24} \\ g_{31} \\ g_{32} \\ g_{34} \\ g_{42} \\ g_{43} \end{bmatrix} - \begin{bmatrix} & & S_{21} & S_{21} & S_{21} & & & & & & \\ & & & & & S_{31} & S_{31} & S_{31} & & & \\ S_{12} & S_{12} & & & & & & & & & \\ & & & & S_{32} & S_{32} & S_{32} & & & & \\ & & & & & & & S_{42} & S_{42} & & \\ S_{13} & S_{13} & & & & & & & & & \\ & & & & S_{23} & S_{23} & S_{23} & & & & \\ & & & & & & & & S_{43} & S_{43} & \\ & & & S_{24} & S_{24} & S_{24} & & & & & \\ & & & & & & & & & & S_{34} & S_{34} & S_{34} \end{bmatrix} = \begin{bmatrix} g_{12} \\ g_{13} \\ g_{21} \\ g_{23} \\ g_{24} \\ g_{31} \\ g_{32} \\ g_{34} \\ g_{42} \\ g_{43} \end{bmatrix} = \begin{bmatrix} b_{12} \\ b_{13} \\ b_{21} \\ b_{23} \\ b_{24} \\ b_{31} \\ b_{32} \\ b_{34} \\ b_{42} \\ b_{43} \end{bmatrix}, \quad (9)$$

The matrix above corresponds to a more general domain decomposition (see Fig. 1), which shows that the sweeping-type algorithms that present in following sections can be applied to more general cases. Considering that the approach [20] based on compatibility relations for right-angle corners reveals to be much more efficient, In Section 4, we only consider checkboard-type domain decompositions.

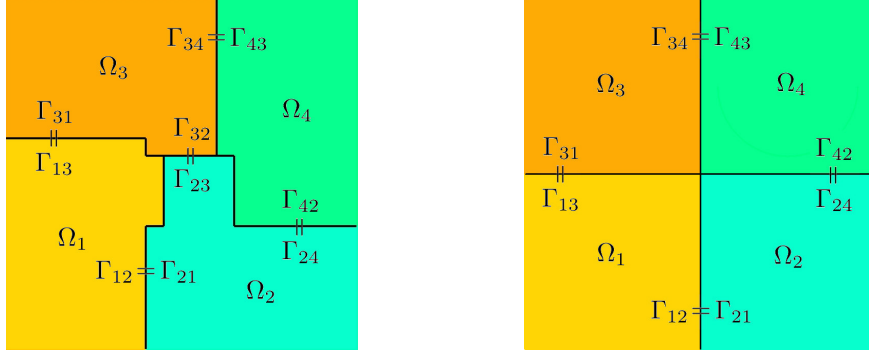


Figure 1: Non-overlapping decompositions with 4 subdomains. The left figure presents a more general domain decomposition, and the right figure presents a checkerboard domain decomposition.

3.2 Iterative algorithm

One efficient iterative algorithm to solve (7) is the GMRES algorithm [23]. Let initial guess $\mathbf{g}^{(0)}$ be given, and orthonormal basis $\mathbf{z}_{\mathbf{m}} \in \mathcal{K}_{\mathbf{m}}$ be constructed using Arnoldi algorithm, the norm of the residual in this orthonormal basis is minimized as follows

$$\min_{\mathbf{z}_{\mathbf{m}} \in \mathcal{K}_{\mathbf{m}}} \|\mathbf{b} - (\mathbf{Id} - \mathbf{S})(\mathbf{g}^{(0)} + \mathbf{z}_{\mathbf{m}})\| = \min_{\mathbf{z}_{\mathbf{m}} \in \mathcal{K}_{\mathbf{m}}} \|\mathbf{r}^{(0)} - (\mathbf{Id} - \mathbf{S})\mathbf{z}_{\mathbf{m}}\|. \quad (10)$$

3.3 Sweeping preconditioners

In this section, we present, in the first place, a tri-diagonal matrix form based on the explicit representation of the interface problem in the case of such block decompositions. Next, we present a family of generalized sweeping preconditioners which covers sweeping preconditioners for layered domain decompositions, and diagonal sweeping preconditioners for checkerboard-type domain decompositions.

3.3.1 Block matrix forms

On the example with 4 subdomains (9), it presents that the iterate operator in the interface problem (7) consists of all local scattering operators S_{ij} . The matrix consisting of these local operators can be reformed as a tridiagonal structure. To do this, we firstly define the subdomains' group

$$\Omega_{[I]} := \left\{ \bigcup_i \Omega_i \text{ for some } i \in \mathbb{D} \right\}.$$

The subdomains is grouped into a finite number N_g such that

$$\Omega_{[I]} \cap \Omega_{[J]} = \emptyset, \quad \text{for } J \neq I, \quad \bigcup_I \Omega_{[I]} = \Omega.$$

Next, we introduce the local scattering operator block

$$\mathbf{S}_{[IJ]} \in \mathcal{M}_{e_{[I]} \times e_{[J]}}(S_{ij}),$$

where $e_{[I]}$ is the number of interfaces of $\Omega_{[I]}$. Finally, the interface problem (7) can be rewritten as

$$\mathbf{g}_{[J]} - \sum_I \mathbf{S}_{[IJ]} \mathbf{g}_{[I]} = \mathbf{b}_{[J]}, \quad \forall J. \quad (11)$$

We represent the example with 4 subdomains (9) below:

$$\left(\mathbf{Id} - \begin{bmatrix} & \mathbf{S}_{[21]} & & \\ \mathbf{S}_{[12]} & \mathbf{S}_{[22]} & \mathbf{S}_{[32]} & \\ & \mathbf{S}_{[23]} & & \end{bmatrix} \right) \begin{bmatrix} \mathbf{g}_{[1]} \\ \mathbf{g}_{[2]} \\ \mathbf{g}_{[3]} \end{bmatrix} = \begin{bmatrix} \mathbf{b}_{[1]} \\ \mathbf{b}_{[2]} \\ \mathbf{b}_{[3]} \end{bmatrix}, \quad (12)$$

with three subdomains' groups $\Omega_{[1]} = \{\Omega_1\}$, $\Omega_{[2]} = \{\Omega_2, \Omega_3\}$, and $\Omega_{[3]} = \{\Omega_4\}$.

The system (11) is a generalized tridiagonal system for the interface problem (7). This generalized system can be further decomposed for designing sweeping-type preconditioners. For instance, if domain partitions are one-dimensional, the corresponding matrix is a block tridiagonal, which was leveraged to device efficient sweeping preconditioners (see *e.g.* [3, 24, 27]). If domain partitions are checkerboard-type, the matrix is a block tridiagonal if the blocks are arranged diagonally with the diagonal of the matrix being identical, which was leveraged to device efficient diagonal sweeping preconditioners (see *e.g.* [9, 18, 25]). If domain partitions are arbitrary, the matrix is still a block tridiagonal with certain subdomains' groups, which can be used to design sweeping preconditioners abandoning certain blocks at diagonals (for example, $\mathbf{S}_{[22]}$ in (12) is abandoned).

We present sweeping preconditioners of the interface problem (7). To be efficient, a preconditioner \mathbf{P} is a kind of matrix that is similar to the original matrix such that the new matrix $\mathbf{P}^{-1}(\mathbf{Id} - \mathbf{S})$ is well-conditioned. A good preconditioner makes the preconditioned problem solved more easily than the unpreconditioned problem. Secondly, the application of the inverse of the preconditioner is affordable. The tridiagonal structure presented above makes the inverse of the preconditioner possible. The lower and upper triangular parts of the tridiagonal matrix can be explicitly inverted.

3.3.2 Symmetric Gauss-Seidel (SGS) preconditioner

With certain subdomains' groups, abandoning the scattering blocks $\mathbf{S}_{[II]}, \forall I$, we obtain a matrix \mathbf{P}_{SGS} of which the diagonal part is an identity matrix. This matrix can then be rewritten as $\mathbf{P}_{\text{SGS}} = \mathbf{L}_{\text{SGS}}\mathbf{U}_{\text{SGS}}$, with the lower triangular matrix

$$\mathbf{L}_{\text{SGS}} = \prod (\mathbf{Id} - \mathbf{S}_{[I-1, I]}), \quad I = 2, \dots, N_g,$$

with the lower triangular matrix

$$\mathbf{U}_{\text{SGS}} = \prod (\mathbf{Id} - \mathbf{S}_{[I, I-1]}), \quad I = N_g, \dots, 2.$$

We can easily invert the matrix $\mathbf{P}_{\text{SGS}}^{-1} = \mathbf{U}_{\text{SGS}}^{-1}\mathbf{L}_{\text{SGS}}^{-1}$, with

$$\begin{aligned} \mathbf{L}_{\text{SGS}}^{-1} &= \prod (\mathbf{Id} - \mathbf{S}_{[I-1, I]})^{-1} \\ &= \prod (\mathbf{Id} + \mathbf{S}_{[I-1, I]}), \quad I = N_g, \dots, 2, \end{aligned}$$

and

$$\begin{aligned} \mathbf{U}_{\text{SGS}}^{-1} &= \prod (\mathbf{Id} - \mathbf{S}_{[I, I-1]})^{-1} \\ &= \prod (\mathbf{Id} + \mathbf{S}_{[I, I-1]}), \quad I = 2, \dots, N_g. \end{aligned}$$

With different subdomains' groups, the preconditioner \mathbf{P}_{SGS} can be different.

3.3.3 Double Sweep (DS) preconditioner

We introduce the forward local scattering operator:

$$\vec{S}_{ij} : x_{ik} \rightarrow (-\partial_{\mathbf{n}_{ij}} - \iota\kappa T)v_i \quad \text{where} \quad \begin{cases} (-\Delta - \kappa^2)v_i = 0, & \text{in } \Omega_i, \\ (\partial_{\mathbf{n}_i} - \iota\kappa)v_i = 0, & \text{on } \partial\Omega_i \cap \Gamma^\infty, \\ (\partial_{\mathbf{n}_{ik}} - \iota\kappa T)v_i = x_{ik}, & \text{on } \Gamma_{ik}, \\ (\partial_{\mathbf{n}_{il}} - \iota\kappa T)v_i = 0, & \text{on } \Gamma_{il}, \forall l \neq k, \end{cases} \quad (13)$$

where $\Omega_i \in \Omega_{[I-1]}$, $\Omega_j \in \Omega_{[I]}$, and $\Omega_k \notin \Omega_{[I]}$, $I = 2, \dots, N_g$. And the backward local scattering operator:

$$\overleftarrow{\mathbf{S}}_{ij} : x_{ik} \rightarrow (-\partial_{\mathbf{n}_{ij}} - \imath\kappa T)v_i \quad \text{where} \quad \begin{cases} (-\Delta - \kappa^2)v_i = 0, & \text{in } \Omega_i, \\ (\partial_{\mathbf{n}_i} - \imath\kappa)v_i = 0, & \text{on } \partial\Omega_i \cap \Gamma^\infty, \\ (\partial_{\mathbf{n}_{ik}} - \imath\kappa T)v_i = x_{ik}, & \text{on } \Gamma_{ik}, \\ (\partial_{\mathbf{n}_{il}} - \imath\kappa T)v_i = 0, & \text{on } \Gamma_{il}, \forall l \neq k, \end{cases} \quad (14)$$

where $\Omega_i \in \Omega_{[I]}$, $\Omega_j \in \Omega_{[I-1]}$, and $\Omega_k \notin \Omega_{[I-1]}$, $I = N_g \dots, 2$. Next, we introduce the forward and backward local scattering operator block

$$\overrightarrow{\mathbf{S}}_{[IJ]} \in \mathcal{M}_{e_{[I]} \times e_{[J]}}(\overrightarrow{\mathbf{S}}_{ij}), \quad \overleftarrow{\mathbf{S}}_{[IJ]} \in \mathcal{M}_{e_{[I]} \times e_{[J]}}(\overleftarrow{\mathbf{S}}_{ij}).$$

In the same way that we have done for the SGS preconditioner, we can obtain the inverse of the DS preconditioner $\mathbf{P}_{\text{DS}}^{-1} = \mathbf{U}_{\text{DS}}^{-1}\mathbf{L}_{\text{DS}}^{-1}$ with

$$\begin{aligned} \mathbf{L}_{\text{DS}}^{-1} &= \prod \left(\mathbf{Id} - \overrightarrow{\mathbf{S}}_{[I-1, I]} \right)^{-1} \\ &= \prod \left(\mathbf{Id} + \overrightarrow{\mathbf{S}}_{[I-1, I]} \right), \quad I = N_g, \dots, 2, \end{aligned}$$

and

$$\begin{aligned} \mathbf{U}_{\text{DS}}^{-1} &= \prod \left(\mathbf{Id} - \overleftarrow{\mathbf{S}}_{[I, I-1]} \right)^{-1} \\ &= \prod \left(\mathbf{Id} + \overleftarrow{\mathbf{S}}_{[I, I-1]} \right), \quad I = 2, \dots, N_g. \end{aligned}$$

The additional property of DS preconditioner is

$$\mathbf{P}_{\text{DS}} = \mathbf{L}_{\text{DS}} + \mathbf{U}_{\text{DS}} - \mathbf{Id}.$$

This shows that the application of $\mathbf{L}_{\text{DS}}^{-1}$ and $\mathbf{U}_{\text{DS}}^{-1}$ can be simultaneous, since the relations below hold:

$$\begin{aligned} \mathbf{P}_{\text{DS}}^{-1} &= \mathbf{L}_{\text{DS}}^{-1}\mathbf{U}_{\text{DS}}^{-1} \\ &= \mathbf{L}_{\text{DS}}^{-1} + \mathbf{U}_{\text{DS}}^{-1} - \mathbf{Id}. \end{aligned}$$

3.4 Block-Jacobi sweeping preconditioners

The SGS and DS preconditioners for checkerboard-type domain decompositions presented in the previous contexts have their inherent parallelism compared to that for layer-type domain decompositions. In the next section, we present snapshots of the solution at different steps of forward and backward sweeps of the first GMRES iterations with the SGS preconditioners (see Fig. 2 and Fig. 3). Observing these snapshots shows how processors perform concurrently at each step of forward and backward sweeps. It also shows that not every processor performs at each step and only a few processors are working parallelly at some steps. The reason is that the steps of the sweeping process on checkerboard-type domain decompositions are still inherently sequential, and the direction of each step of the sweep is perpendicular to the subdomains' diagonal limiting the parallelism. Another explanation could be that this limited amount of parallelism is extracted from the complete LU factorization. Using this kind of preconditioner provides good intrinsic qualities but a limited degree of parallelism. Some alternative techniques are suitable to increase parallelism. A good approach is block-Jacobi preconditioning. Although this preconditioning is often considered to be not very useful because the rate of convergence of the resulting iteration tends to be much larger than the original variants, we show this technique is well suitable for sweeping-type algorithms, which increase parallelism and at the same time maintain good intrinsic preconditioning qualities.

The idea of the block-Jacobi preconditioner is simple: the original preconditioner is replaced by its block-diagonal. Applying this technique to the sweeping-type preconditioners, we obtain block-Jacobi sweeping preconditioners. The new variants can be interpreted as several partial sweeps, which can be performed independently and concurrently.

Considering a $N_x \times N_y$ ($N_x \geq N_y$) checkerboard partition with row-based assignments (there are N_y processors), in the interface problem (11), $J = 1, 2, \dots, N_x + N_y - 1$. And the number of Jacobi blocks is $p = \lfloor N_y/N_x \rfloor + 1$. For each Jacobi block, its location in the original problem (11) is

$$\begin{aligned} 1 + (i-1)N_x &\leq J \leq 1 + iN_x, & i = 1, 2, \dots, p-1, \\ 1 + (i-1)N_x &\leq J \leq N_x + N_y - 1, & i = p. \end{aligned}$$

The matrix of this block-Jacobi preconditioner with starting number J and ending number J for each Jacobi block \mathbf{J}_i is:

$$\left[\begin{array}{c} \mathbf{J}_1 \\ \mathbf{J}_2 \\ \dots \\ \mathbf{J}_{p-1} \\ \mathbf{J}_p \end{array} \right] \begin{array}{l} \rightarrow J = 1 \\ \rightarrow J = 1 + N_x \\ \rightarrow J = 1 + 2N_x \\ \rightarrow J = 1 + (p-2)N_x \\ \rightarrow J = 1 + (p-1)N_x \\ \rightarrow J = N_x + N_y - 1 \end{array} \quad (15)$$

From (15), one observes that the block-Jacobi matrix corresponding to these partial sweeps is derived from the original sweeping-type preconditioner matrix, where one identity block matrix is overlapped by two blocks. Although there is an overlap of two blocks corresponding to two partial sweeps, there is no communication between two neighboring partial sweeping domains. The reason is that these partial sweeps start at the same time. When one partial sweep goes to the end (which is the starting part of the next neighboring partial sweeping domain), the next partial sweep has already gone to its end, thus it doesn't affect the next partial sweep.

4 Numerical results

In this part, the block-Jacobi sweeping preconditioners are studied and compared to the full sweeping preconditioners by considering several two- and three-dimensional benchmarks with a high-order finite element method. The following benchmarks are considered: a scattering model in 2D (4.1), the Marmousi model (4.2) and a scatter model in 3D (4.3). The proposed approaches and the computational results presented in this paper are implemented in parallel by Message Passing Interface (MPI) on a single multi-core computer. The local sub-problems in sub-domains are solved by sparse direct solver PARDISO [1, 4, 5]. The mesh generation, mesh decomposition, and post-processing are credited by Gmsh [17]. The preconditioned optimized Schwarz method has been implemented in a dedicated research code¹ written in C.

Implementing the approach using MPI, we assign each row or column of subdomains to one MPI rank. In terms of preconditioned optimized Schwarz methods, each local sub-problem is solved twice at each iteration of GMRES: the one at the level of matrix-free product, the other at the level of preconditioning procedure. If we assign each subdomain to one MPI rank, the sequential nature of sweeping preconditioners limits the efficiency of the approach. At the level of matrix-free product, every MPI rank can solve its local sub-problem concurrently within one iteration. At the level of the preconditioning procedure, sweeps must be done in a sequence of steps, which, from a time measurement perspective, corresponds to $2(N_x + N_y - 1)$ iterations in two-dimensional cases and $2(N_x + N_y + N_z - 1)$ iterations. Thus, within the scope of the preconditioning procedure, there are a lot of wasted computing resources and increased computing time if one chooses to assign each local problem to one MPI rank. On the contrary, if we

¹Repository: <https://git.immc.ucl.ac.be/rdai/hxtddm.git>.

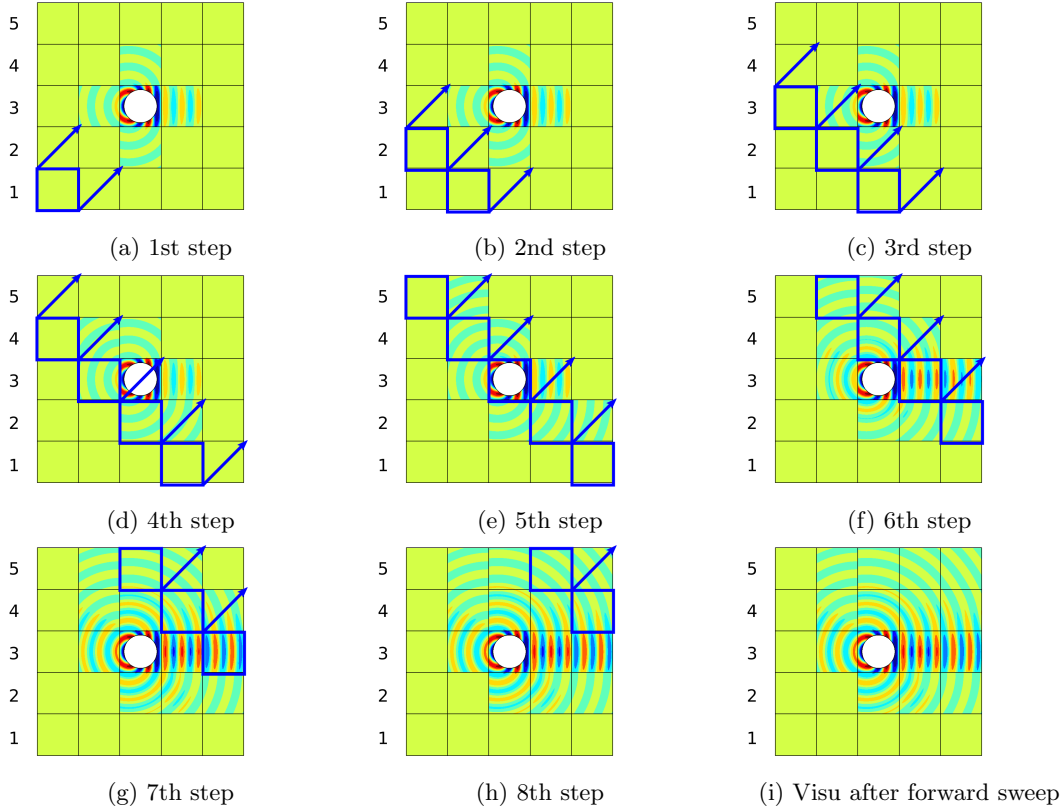


Figure 2: Scattering model in 2D. Snapshot of the solution at different steps of forward sweep of 1st GMRES iteration with the full sweeping preconditioner. The numbers at left side are processors' identities. Each row of subdomains is assigned to one MPI rank. Subdomains processed in parallel have same blue color.

assign each row or column of subdomains to one MPI rank, the steps of traversing all subdomains at the level of the matrix-free product are equivalent to the steps of the sweeping preconditioning procedure, which allows one to obtain a parallel scalable preconditioned solver.

In conclusion, the parallelism of our approach is realized by assigning subdomains to MPI ranks in a row- or column-based fashion such that the i -th row or column of the checkerboard domain decomposition is processed by rank i .

4.1 Scattering model in 2D

We start by describing the validation case used in this subsection. The test case is a homogeneous scattering problem in free space within a rectangle geometry ($\Omega = [-1.25, 2.50 \cdot N_x - 1.25] \times [-1.25, 2.50 \cdot N_y - 1.25]$), which is decomposed into $N_x \times N_y = 5 \times 5$, 5×10 , and 5×15 rectangular subdomains. An incident plane wave is generated by a sound-soft circular cylinder of radius equal to 1 which is located at the Origin. On the circular cylinder, the Dirichlet boundary condition $u(\mathbf{x}) = -\exp^{ikx}$ is prescribed at the boundary of the sound-soft scatterer. The Padé-type HABC is prescribed on the exterior boundaries and the interior boundaries used as the absorbing boundary conditions and the transmission boundary conditions, respectively. The compatibility conditions are prescribed at the corners and the cross-points treatment is prescribed at the cross-points. We employ the Padé-type HABC operator with a large number of auxiliary fields, which improves the efficiency of the DD methods for scattering problems, to show distinct residual history of GMRES. The parameters of the HABC operator are $N = 8$ and $\phi = \pi/3$.

We use a standard high-order finite element method to solve this problem. The meshes used by the method are made of high-order triangles which are generated by Gmsh [17]. The following numerical setting are considered: $P7$ finite elements with 3 elements per wavelength ($h \approx 1/21$). The meshes of

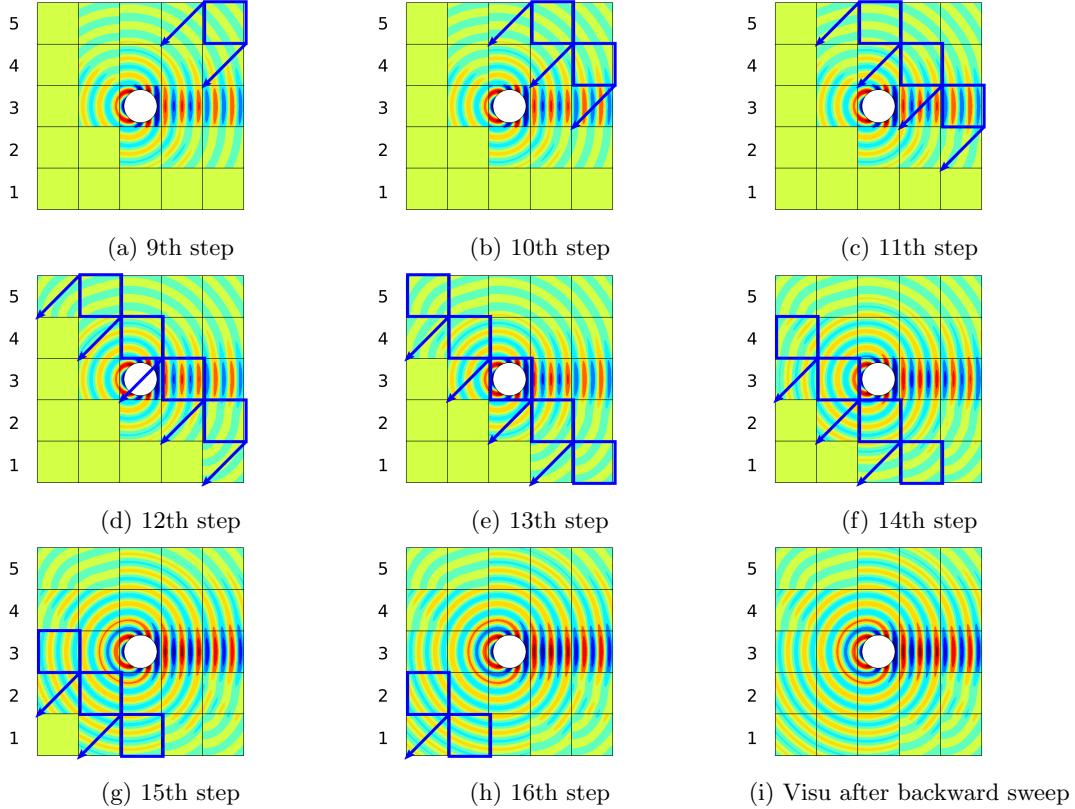


Figure 3: Scattering model in 2D. Snapshot of the solution at different steps of backward sweep of 1st GMRES iteration with the full sweeping preconditioner. The numbers at left side are processors' identities. Each row of subdomains is assigned to one MPI rank. Subdomains processed in parallel have same blue color.

three partitions are made of 99023 nodes, 4016 $P7$ triangles (for $N_x \times N_y = 5 \times 5$ partition), 198479 nodes, 8064 $P7$ triangles (for $N_x \times N_y = 5 \times 10$ partition), and 297935 nodes, 12112 $P7$ triangles (for $N_x \times N_y = 5 \times 15$ partition), respectively.

Fig. 2 and 4 show snapshots of the solutions at different steps of forward sweep (sweep starts from the bottom-left corner to the top-right corner) of the 1st GMRES iteration with different sweeping preconditioners. The solution is already good at each step for these two preconditioners. The HABC operator with a large number of auxiliary fields used in the transmission conditions gives high-fidelity values at transmission boundaries for sub-problems in sub-domains. Although the forward sweep in Fig. 2 goes through the whole computational domain from the bottom-left corner to the top-right corner, it takes 8 steps. If we take the backward sweep into account, there are 16 steps of the preconditioning procedure at each iteration. In the second situation, it only takes 5 steps in the forward partial sweeps (see Fig. 4).

Fig. 6, 7, and 8 show snapshots of the solutions and residual histories of GMRES with the different preconditioners for three partitions. All forward/backward (partial) sweeps of these preconditioners start from the bottom-left/top-left to the top-right/bottom-left. The violet boxes indicate the cut location which separates partial sweeps. For instance, in Fig. 6, two forward partial sweeps in the block-Jacobi preconditioner start from the bottom-left corner to the violet boxes and from the violet boxes to the top-right corner, respectively.

The residual histories obtained with the two different preconditioners for three partitions are shown, as well. In Fig. 6, the relative residual suddenly drops in residual at the first iteration when a full sweeping preconditioner is used. With the block-Jacobi sweeping preconditioner used, it happens at the second iteration, which corresponds to the number of partial sweeps, that is to say, there are two partial sweeps. If Fig. 7 and 8, the histories of the relative residual are similar. With two cuts, which corresponds to three partial sweeps, it takes two more iterations to reach the sudden drop compared to

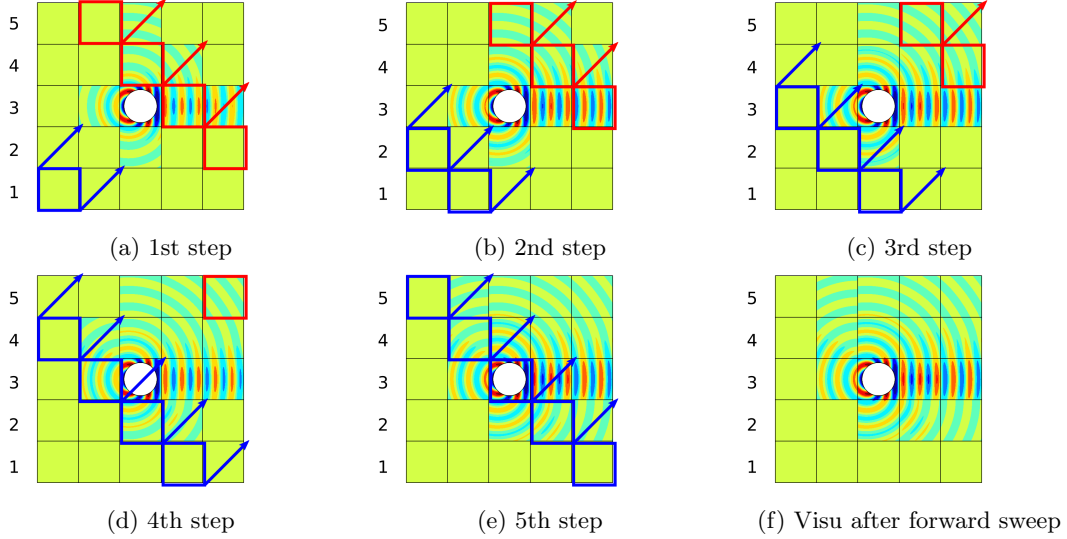


Figure 4: Scattering model in 2D. Snapshot of the solution at different steps of forward sweep of 1st GMRES iteration with the block-Jacobi sweeping preconditioner. The numbers at left side are processors' identities. Each row of subdomains is assigned to one MPI rank. Subdomains processed in parallel have same blue and red color, which represent two partial sweeps.

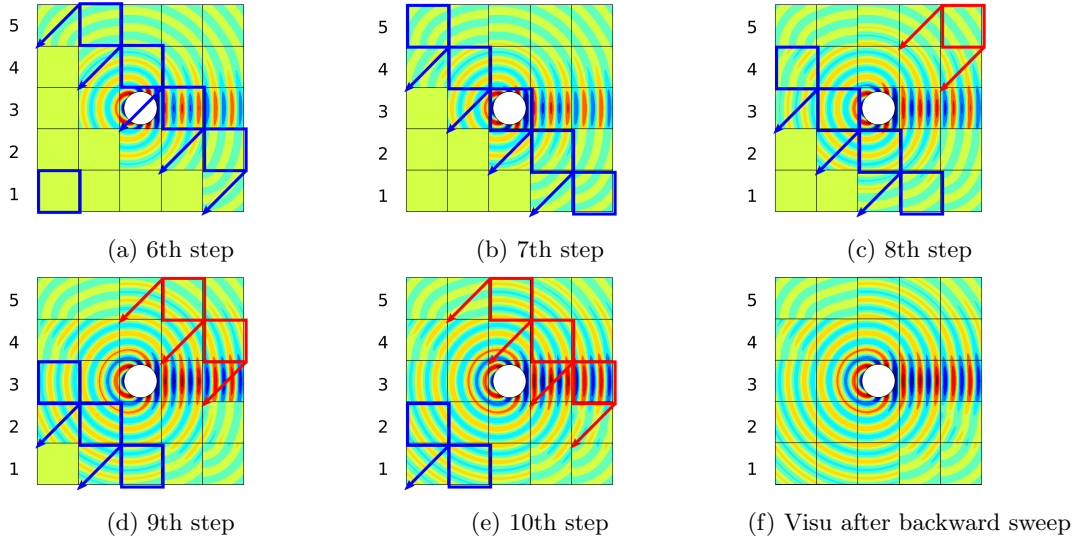


Figure 5: Scattering model in 2D. Snapshot of the solution at different steps of backward sweep of 1st GMRES iteration with the block-Jacobi sweeping preconditioner. The numbers at left side are processors' identities. Each row of subdomains is assigned to one MPI rank. Subdomains processed in parallel have same blue and red color, which represent two partial sweeps.

the history with the full sweeping preconditioner used. Similarly, with three cuts (four partial sweeps), it takes three more iterations to reach the sudden drop.

4.2 Marmousi model

The Marmousi model is a complex 2D structural model which involves strong horizontal and vertical velocity changes (see Fig. 9). The performance of numerical solvers is always evaluated by this heterogeneous model. The system (1) is solved over the rectangular domain $[0, 9192] \times [0, -2904]$, with the HABC prescribed on the boundary of the domain. There is one point source placed at coordinate

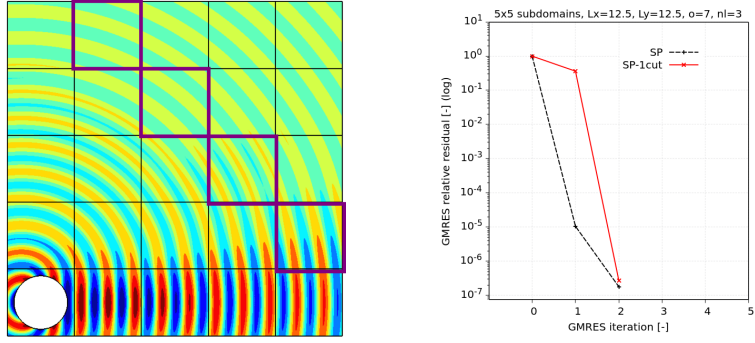


Figure 6: Scattering model in 2D. The computational domain is decomposed into $N_x \times N_y = 5 \times 5$. Residual history with sweeping preconditioner (SP) and block-Jacobi preconditioner with one cut (SP-1cut).

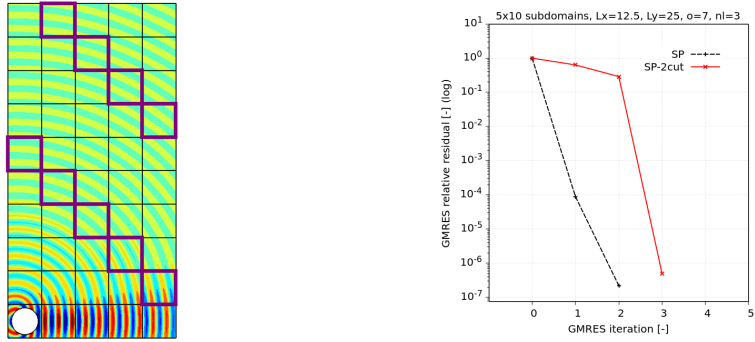


Figure 7: Scattering model in 2D. The computational domain is decomposed into $N_x \times N_y = 5 \times 10$. Residual history with sweeping preconditioner (SP) and block-Jacobi preconditioner with one cut (SP-2cut).

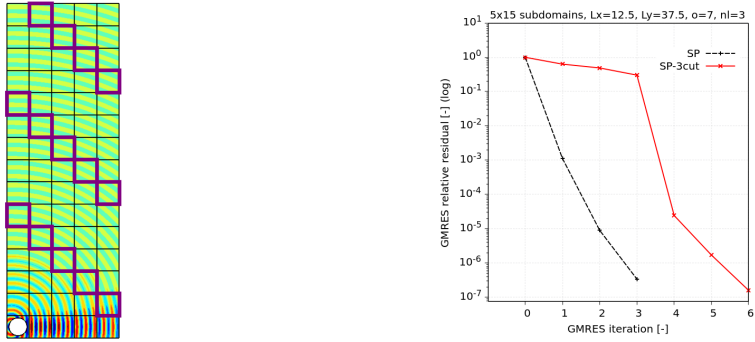


Figure 8: Scattering model in 2D. The computational domain is decomposed into $N_x \times N_y = 5 \times 15$. Residual history with sweeping preconditioner (SP) and block-Jacobi preconditioner with one cut (SP-3cut).

$(9192 \times 7/8, -10)$. The angular frequency increases as the number of subdomains increases, and the wavenumber $k(\mathbf{x})$ is equal to $\omega/c(\mathbf{x})$.

The numerical setting is $P1$ triangular elements with 10 mesh vertices per wavelength. The mesh of the computational domain is made of 117172 nodes and 25878 $P1$ triangles for $N_x \times N_y = 6 \times 2$ partition and $\omega = 2\pi \times 10$, 461467 nodes and 102228 $P1$ triangles for $N_x \times N_y = 12 \times 4$ partition and $\omega = 2\pi \times 20$, 1.83713e+06 nodes and 407610 $P1$ triangles for $N_x \times N_y = 24 \times 8$ partition and $\omega = 2\pi \times 30$, and 7.33885e+06 nodes and 1.62958e+06 $P1$ triangles for $N_x \times N_y = 48 \times 16$ partition and $\omega = 2\pi \times 40$. The parameters of the HABC operator are $N = 4$ and $\phi = \pi/3$ for both the exterior boundary conditions

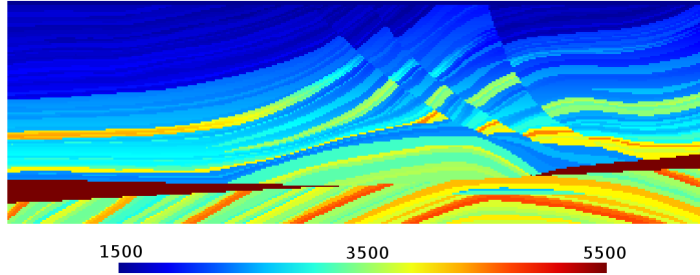


Figure 9: Marmousi model. Velocity profile with values from 1500 m/s to 5500 m/s.

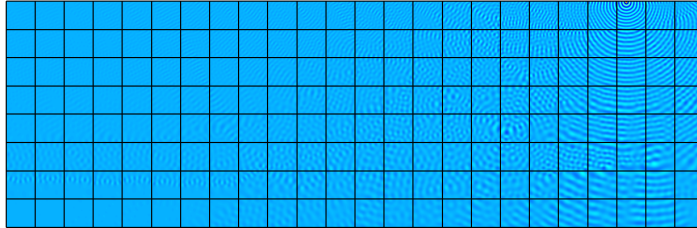


Figure 10: Marmousi model. Numerical solution and domain partition with $N_x \times N_y = 24 \times 8$.

ω	$N_x \times N_y$	SP (iters)	SP (timing)	SP-cut (iters)	SP-cut (timing)
$2\pi \times 10$	6×2	10	1.0s	12	0.5s
$2\pi \times 20$	12×4	17	3.9s	22	1.9s
$2\pi \times 40$	24×8	27	13.5s	33	6.4s
$2\pi \times 80$	48×16	47	53.9s	50	24.0s

Table 1: Marmousi model: Number of iterations and runtime in seconds with the two different preconditioners for different domain partitions and angular frequencies.

and the transmission conditions. A snapshot of the numerical solution for the Marmousi model is shown in Fig. 10.

The number of GMRES iterations and the runtime to reach a relative residual 10^{-6} with the two different preconditioners are given in Table 1. The runtime corresponds to the GMRES resolution phase. Comparing all the cases with the two different preconditioners, the DDMs with block-Jacobi preconditioners perform better. The runtime with block-Jacobi sweeping preconditioners is always less than that with full sweeping preconditioners. Although the number of partial sweeps is different with different domain decomposition configurations, the number of iterations with block-Jacobi sweeping preconditioners is always slightly larger than that with full sweeping preconditioners, which coincides the conclusion in [28]: the number of iterations remains constant for sweep lengths as short as certain subdomains' groups.

4.3 Scattering model in 3D

The last test case is a homogeneous scattering problem in free space in 3D within a cubic geometry. We consider an incident plane wave by a sound-soft sphere of radius equal to 1 which is located at the Origin. The scattered field is computed in a three-dimensional cubic domain of size $7.5 \times 7.5 \times 7.5$, which is partitioned into $3 \times 3 \times 3$ cubic subdomains.

The Dirichlet boundary condition $u(\mathbf{x}) = -\exp^{ik \cdot \mathbf{x}}$ is prescribed on the boundary of the sphere, and the Padé-type HABC is prescribed on the exterior boundary and the transmission boundaries, with compatibility conditions on the exterior edges and corners, and cross-point treatments on the interior edges and corners. The number of auxiliary fields $N = 4$ and the parameter $\phi = \pi/3$ are used for both

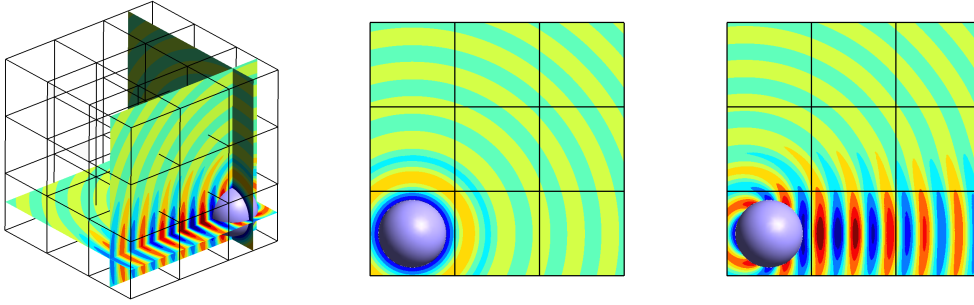


Figure 11: Scattering model in 3D. Numerical solution (general visualisation, +X view, and +Z view) and domain partition with $3 \times 3 \times 3$ subdomains.

ω	$N_x \times N_y \times N_z$	SP (iters)	SP (timing)	SP-cut (iters)	SP-cut (timing)
$2\pi \times 1$	$3 \times 3 \times 3$	11	15.8s	13	10.0s
$2\pi \times 2$	$3 \times 3 \times 3$	11	92.8s	12	55.7s
$2\pi \times 3$	$3 \times 3 \times 3$	11	450.2s	13	272.1s

Table 2: Scattering model in 3D: Number of iterations and runtime in seconds with the two different preconditioners for different domain partitions and angular frequencies.

exterior and interior boundary conditions. The wavenumber $||\kappa||$ is equal to 2π , 4π , and 6π for three cases, with direction $[1/2, 1/2, 0]$. We use a tetrahedral mesh with 3 $P3$ finite elements per wavelength, resulting in 333419 nodes and 69686 $P3$ tetrahedra for $\omega = 2\pi \times 1$, 2.02266e+06 nodes and 435825 $P3$ tetrahedra for $\omega = 2\pi \times 2$, and 6.87676e+06 nodes and 1.49914e+06 $P3$ tetrahedra for $\omega = 2\pi \times 3$.

The number of iterations and the runtime to reach a relative residual 10^{-6} with the two different preconditioners are given in Table 2. The runtime corresponds to the GMRES resolution phase.

In this case, we study the efficiency of the block-Jacobi sweeping preconditioners concerning the angular frequency ω . We observe that the influence of angular frequency ω on the rate of convergence is not significant for the block-Jacobi sweeping preconditioners. And we also get similar results that the DDMs with block-Jacobi preconditioners perform better with less time consumption. The number of iterations with block-Jacobi sweeping preconditioners is slightly larger than that with full sweeping preconditioners as angular frequency increases.

Three snapshots of the numerical solution for the scattering model in 3D are shown in Fig. 11.

5 Conclusion

In this work, we have proposed block-Jacobi sweeping preconditioners for non-overlapping OS methods applied to Helmholtz problems with checkerboard-type domain decomposition in two and three dimensions by assigning subdomains to MPI ranks in a row- or column-based fashion. There are similar preconditioners proposed in [28] for layer-type domain decompositions, where the transmission operators corresponding to the cut domain are replaced by 0 to forbid communication between two partial sweeping domains. Alternatively, in this work, we consider overlapping block-Jacobi sweeping preconditioners. They are the new variants of multidirectional sweeping preconditioners originally proposed in [9], in which partial sweeps are introduced to reduce the number of steps in the preconditioning procedure and increase the parallel efficiency to achieve some speed-up over the optimized Schwarz methods. With row- or column-based fashion, partial sweeps can be performed concurrently with the full usage of the resources at each step of the block-Jacobi sweeping preconditioners. The proposed block-Jacobi sweeping algorithms can also be applied to the Maxwell equations, in 2D and 3D, because of their independency from underlying problem formulation. However, the cross-point treatments are not available for high-order transmission conditions, which might limit the accuracy and efficiency of the block-Jacobi sweeping preconditioners.

References

- [1] C. Alappat, A. Basermann, A. R. Bishop, H. Fehske, G. Hager, O. Schenk, J. Thies, and G. Wellein. A recursive algebraic coloring technique for hardware-efficient symmetric sparse matrix-vector multiplication. *ACM Trans. Parallel Comput.*, 7(3), June 2020.
- [2] P. Amestoy, R. Brossier, A. Buttari, J.-Y. L'Excellent, T. Mary, L. Métivier, A. Miniussi, and S. Operto. Fast 3d frequency-domain full-waveform inversion with a parallel block low-rank multifrontal direct solver: Application to obc data from the north sea3d fd fwi with blr direct solver. *Geophysics*, 81(6):R363–R383, 2016.
- [3] A. V. Astaneh and M. N. Guddati. A two-level domain decomposition method with accurate interface conditions for the Helmholtz problem. *International Journal for Numerical Methods in Engineering*, 107(1):74–90, 2016.
- [4] M. Bollhöfer, A. Eftekhari, S. Scheidegger, and O. Schenk. Large-scale sparse inverse covariance matrix estimation. *SIAM Journal on Scientific Computing*, 41(1):A380–A401, 2019.
- [5] M. Bollhöfer, O. Schenk, R. Janalik, S. Hamm, and K. Gullapalli. State-of-the-art sparse direct solvers. pages 3–33, 2020.
- [6] Y. Boubendir, X. Antoine, and C. Geuzaine. A quasi-optimal non-overlapping domain decomposition algorithm for the Helmholtz equation. *Journal of Computational Physics*, 231(2):262–280, 2012.
- [7] Z. Chen and X. Xiang. A source transfer domain decomposition method for helmholtz equations in unbounded domain. *SIAM Journal on Numerical Analysis*, 51(4):2331–2356, 2013.
- [8] P.-H. Cocquet and M. J. Gander. How large a shift is needed in the shifted helmholtz preconditioner for its effective inversion by multigrid? *SIAM Journal on Scientific Computing*, 39(2):A438–A478, 2017.
- [9] R. Dai, A. Modave, J.-F. Remacle, and C. Geuzaine. Multidirectional sweeping preconditioners with non-overlapping checkerboard domain decomposition for helmholtz problems. *Journal of Computational Physics*, page 110887, 2022.
- [10] B. Després. Méthodes de décomposition de domaine pour les problèmes de propagation d’ondes en régime harmonique. *These, Université Paris IX Dauphine, UER Mathématiques de la Décision*, 1991.
- [11] B. Després, A. Nicolopoulos, and B. Thierry. Corners and stable optimized domain decomposition methods for the helmholtz problem. *Numerische Mathematik*, 149(4):779–818, 2021.
- [12] B. Engquist and L. Ying. Sweeping preconditioner for the helmholtz equation: hierarchical matrix representation. *Communications on pure and applied mathematics*, 64(5):697–735, 2011.
- [13] B. Engquist and L. Ying. Sweeping preconditioner for the Helmholtz equation: moving perfectly matched layers. *Multiscale Modeling & Simulation*, 9(2):686–710, 2011.
- [14] Y. A. Erlangga, C. Vuik, and C. W. Oosterlee. On a class of preconditioners for solving the helmholtz equation. *Applied Numerical Mathematics*, 50(3-4):409–425, 2004.
- [15] M. Gander, F. Magoules, and F. Nataf. Optimized Schwarz methods without overlap for the Helmholtz equation. *SIAM Journal on Scientific Computing*, 24(1):38–60, 2002.
- [16] M. J. Gander, I. G. Graham, and E. A. Spence. Applying gmres to the helmholtz equation with shifted laplacian preconditioning: what is the largest shift for which wavenumber-independent convergence is guaranteed? *Numerische Mathematik*, 131(3):567–614, 2015.
- [17] C. Geuzaine and J.-F. Remacle. Gmsh: A 3-D finite element mesh generator with built-in pre-and post-processing facilities. *International journal for numerical methods in engineering*, 79(11):1309–1331, 2009.
- [18] W. Leng and L. Ju. Trace transfer-based diagonal sweeping domain decomposition method for the helmholtz equation: Algorithms and convergence analysis. *Journal of Computational Physics*, 455:110980, 2022.
- [19] P.-L. Lions. On the schwarz alternating method. iii: a variant for nonoverlapping subdomains. In *Third international symposium on domain decomposition methods for partial differential equations*, volume 6, pages 202–223. SIAM Philadelphia, 1990.
- [20] A. Modave, C. Geuzaine, and X. Antoine. Corner treatments for high-order local absorbing boundary conditions in high-frequency acoustic scattering. *Journal of Computational Physics*, 401:109029, 2020.
- [21] A. Modave, A. Royer, X. Antoine, and C. Geuzaine. A non-overlapping domain decomposition method with high-order transmission conditions and cross-point treatment for Helmholtz problems. *Computer Methods in Applied Mechanics and Engineering*, 368:113162, 2020.
- [22] É. Parolin. *Non-overlapping domain decomposition methods with non-local transmission operators for harmonic wave propagation problems*. PhD thesis, Institut Polytechnique de Paris, 2020.
- [23] Y. Saad and M. H. Schultz. GMRES: A generalized minimal residual algorithm for solving nonsymmetric linear systems. *Journal on Scientific and Statistical Computing*, 7(3):856–869, 1986.
- [24] C. C. Stolk. A rapidly converging domain decomposition method for the Helmholtz equation. *Journal of*

- Computational Physics*, 241:240–252, 2013.
- [25] M. Taus, L. Zepeda-Núñez, R. J. Hewett, and L. Demanet. L-sweeps: A scalable, parallel preconditioner for the high-frequency helmholtz equation. *Journal of Computational Physics*, 420:109706, 2020.
 - [26] A. Toselli and O. Widlund. *Domain decomposition methods-algorithms and theory*, volume 34. Springer Science & Business Media, 2006.
 - [27] A. Vion and C. Geuzaine. Double sweep preconditioner for optimized Schwarz methods applied to the Helmholtz problem. *Journal of Computational Physics*, 266:171–190, 2014.
 - [28] A. Vion and C. Geuzaine. Improved sweeping preconditioners for domain decomposition algorithms applied to time-harmonic Helmholtz and Maxwell problems. *ESAIM: Proceedings and Surveys*, 61:93–111, 2018.
 - [29] S. Wang, M. V. de Hoop, J. Xia, and X. S. Li. Massively parallel structured multifrontal solver for time-harmonic elastic waves in 3-d anisotropic media. *Geophysical Journal International*, 191(1):346–366, 2012.
 - [30] L. Zepeda-Núñez and L. Demanet. The method of polarized traces for the 2D Helmholtz equation. *Journal of Computational Physics*, 308:347–388, 2016.
 - [31] L. Zepeda-Núñez and L. Demanet. Nested domain decomposition with polarized traces for the 2D Helmholtz equation. *SIAM Journal on Scientific Computing*, 40(3):B942–B981, 2018.